Journal of Hydrology 635 (2024) 131234

Contents lists available at ScienceDirect

Journal of Hydrology

journal homepage: www.elsevier.com/locate/jhydrol

Research papers

Effects of inter-basin transfers on watershed hydrology and vegetation greening in a large inland river basin

Lin Wang [a,b], Wei Wei [a,b,c,*], Ge Sun [d], Bojie Fu [a,b], Liding Chen [a,b], Xiaoming Feng [a,b], Philippe Ciais [e], Bhaskar Mitra [f], Lixin Wang [g]

[a] State Key Laboratory of Urban and Regional Ecology, Research Center for Eco-environmental Sciences, Chinese Academy of Sciences, Beijing 100085, China
[b] University of Chinese Academy of Sciences, Beijing 100049, China
[c] National Observation and Research Station of Earth Critical Zone on the Loess Plateau in Shaanxi, Xi'an 710061, China
[d] Eastern Forest Environmental Threat Assessment Center, Southern Research Station, USDA Forest Service, Research Triangle Park, NC 27709, USA
[e] Laboratoire des Sciences du Climat et de l'Environnement, IPSL-LSCE, CEA-CNRS-UVSQ-UPSACLAY, Gif sur Yvette, France
[f] Information and Computational Science, James Hutton Institute, Aberdeen, Scotland, United Kingdom
[g] Department of Earth and Environmental Sciences, Indiana University Indianapolis, IN 46202, USA

ARTICLE INFO

This manuscript was handled by A. Bardossy, Editor-in-Chief, with the assistance of Roger Moussa, Associate Editor

Keywords:
Water transfer
Hydrological response
Water balance
Vegetation recovery
Dryland watershed

ABSTRACT

The effects of inter-basin transfers (IBTs) on watershed hydrological balances and associated ecosystem processes remain poorly understood in arid regions because of data scarcity and the complexity of ecosystem responses to water management in many parts of the world. To fill this gap, the objective of this study was to quantify the effect of IBTs on watershed hydrological regimes and the associated vegetation dynamics. We conducted a case study on the Shiyang River Basin, a typical mountain-oasis-desert inland river basin in northwestern China, using water balance and wavelet analysis methods. Long-term (1980–2020) monitoring data from river discharge and groundwater tables were used to construct the water balances and quantify the periodicity of the surface water and groundwater. We observed that over 2.90 billion m^3 of transferred water during 2003–2020 mitigated the declining trend in groundwater, resulting in a change in water storage trend from –91.9 mm/y to –53.7 mm/y. IBTs contributed approximately 230 % of the increase in observed river runoff, 21 %–60 % (42 % on average) of the increase in total water storage, and 1 %–32 % (12 % on average) of the evapotranspiration deficit (i.e., the portion of actual evapotranspiration beyond climate-driven evapotranspiration). IBTs also significantly altered the seasonal fluctuation and periodicity of river flows and groundwater. Increased water availability promoted vegetation recovery and resulted in multiscale resonance periodicities with vegetation, ranging from monthly to interannual scales. Our results indicate that IBTs markedly modified the water cycle, hydrological regimes, and ecosystem processes in the study basin. Thus, we call for long-term monitoring of the timing, frequency, and magnitude of ecohydrological modifications from IBTs to provide critical information for effective watershed management policies to achieve long-term sustainable development in water-stressed regions.

1. Introduction

To satisfy escalating water demand, anthropogenic activities such as water transfers, dam construction, and agricultural irrigation have altered almost every watershed on Earth directly or indirectly (Abbott et al., 2019). This is particularly true for arid regions, where hydraulic engineering activities have exerted a more pronounced influence on the water cycle than climate change (Abbott et al., 2019; Taylor et al., 2013; Wang et al., 2022). To address water shortages, almost all countries have implemented or are planning to implement inter- and intra-basin transfers (IBTs) (Duan et al., 2022; Higgins et al., 2018; Pigram, 2000). IBTs are estimated to redistribute 1.2 % of renewable water resources worldwide, and the cumulative transferred water volume is projected to reach 1910 km^3 by 2050, accounting for approximately 48 % of the total global withdrawal (Shiklomanov, 2000; Shumilova et al., 2018).

IBTs can significantly alter the components of the watershed water cycle within a basin (Chauhan et al., 2023). For instance, IBTs change river flows by affecting hydraulic parameters including the area, water

* Corresponding author at: State Key Laboratory of Urban and Regional Ecology, Research Center for Eco-environmental Sciences, Chinese Academy of Sciences, Beijing 100085, China.
E-mail address: weiwei@rcees.ac.cn (W. Wei).

https://doi.org/10.1016/j.jhydrol.2024.131234
Received 5 January 2024; Received in revised form 31 March 2024; Accepted 2 April 2024
Available online 18 April 2024

Nomenclature

ANUSPLIN	A meteorological interpolation software based on spline functions developed by the Australian National University
CQ	Main downstream water-receiving hydrology gauging station named Caiqi
ET_{clim}	Natural climate-determined estimates of actual evapotranspiration
ET_{defi}	Actual evapotranspiration minus climate-determined evapotranspiration
ET_{GREAM}	Evapotranspiration estimate from Global Land Evaporation Amsterdam Model v3.3a
ET_{TC}	Evapotranspiration estimated from TerraClimate
ET_{CR}	Evapotranspiration based on complementary relationship
ET_{WB}	Water-balance-constrained evapotranspiration
HYS	Reservoir downstream of CQ named Hongyashan Reservoir
IBTs	Inter- and intra-basin transfers
JCX	Downstream hydrographic station with water transfer input named Jichuanxia
JDII	Inter-basin transfer named the Jingtaichuan Electric Power Irrigation Project Phase II
PET	Potential evapotranspiration
SRB	The Shiyang River Basin
XDH	Upstream hydrology gauging station with water transfer input named Xidahe
XYP	Intra-basin transfer named the Xiying River special canal project
YLJJ	Inter-basin transfer named Yin-Liu-Ji-Jin
ZMS	Upstream hydrology gauging station named Zamusi
Indices	
NDVI	Normalized Difference Vegetation Index
Variables	
AET	Actual evapotranspiration
E	Water transfer efficiency
ΔG	Changes in groundwater
P	Precipitation
RI	Runoff input from the midstream to the downstream
RO	Runoff at the watershed outlet
S_y	Specific yield
ΔS	Changes in water storage
ΔSM	Changes in water moisture
$IBT_{receiving}$	Actual amount of water received
$IBT_{providing}$	Amount of water supplied by water-providing areas
ΔWT	Changes in water table

depth, and flow velocity; thus, groundwater recharge as shallow groundwater along rivers interacts with surface water (Yuan et al., 2020; Zhang et al., 2010). Recent studies have revealed an enhancement in irrigation from the transferred water in relative to the increased evapotranspiration and decreased net water flux (precipitation minus evapotranspiration) (Jaramillo and Destouni, 2015; Shibuo et al., 2007). These hydrological alterations subsequently affect the terrestrial water cycle and regional climate (Chauhan et al., 2023; Huntington, 2006). Small but persistent changes in the water balance may have substantial ecological repercussions. (Kuriqi et al., 2020; Rohde et al., 2021). However, previous studies have primarily focused on alterations in individual hydrological components. There remains a gap in quantifying the impact of IBTs on the water cycle in water-balance-constrained basins. One contributing factor is the presence of significant uncertainties in all components of the water balance at the watershed scale (Kampf et al., 2020). As an illustration, in numerous previous studies, the water storage change has often been assumed to be zero to simplify the water balance, presuming that human interference is negligible (Destouni et al., 2013; Jaramillo and Destouni, 2015). However, changes in water storage are crucial to the annual water balance, because they directly influence the allocation of runoff and evapotranspiration, especially in arid regions (Hickel and Zhang, 2006). Moreover, hydrological models and remote sensing products may exhibit considerable bias (de Vrese and Hagemann, 2018; Richey et al., 2015). Therefore, while observation-based studies on the effects of IBTs on changes in the water balance are important, such studies remain challenging.

Existing studies indicate that IBTs typically augment streamflow during peak consumptive demands, such as during the irrigation period in the dry season, whereas diminishing streamflow during wetter periods is characterized by lower consumptive needs (Rolls and Bond, 2017). This can result in markedly irregular streamflow, and even a complete reversal of the seasonal pattern in some cases (Pal and Talukdar, 2020; Rolls and Bond, 2017). The interannual and seasonal dynamics of groundwater play crucial roles in water resource management and ecosystem stability, as groundwater is a vital water source for both humans and vegetation, especially in arid regions (Condon et al., 2020; Jasechko et al., 2014). Changes in surface water and groundwater regimes can impact river networks, community structure and diversity, and ecosystem processes, which has prompted heightened attention to alterations in hydrological regimes (Chen et al., 2010; Palmer and Ruhi, 2019). The responses of hydrological processes to IBTs are time-scale dependent and time-varying (Zhang et al., 2022). For example, the seasonal water balance can influence variations in water flow across a broad spectrum of time scales, ranging from daily to interannual, and it undergoes changes in response to both climate change and management operations (Berghuijs et al., 2014; Guo et al., 2022). IBTs, which are characterized by a spatiotemporal span and dynamic management, are anticipated to influence hydrological regimes across various time scales.

The ecological impacts of alterations in hydrological regimes due to IBTs are multifaceted and variable, encompassing modifications in ecological heterogeneity, biodiversity, floodplain fisheries, and ecosystem services (Lynch et al., 2011; Lytle and Poff, 2004). For example, in the Tarim River Basin in western China, the erratic annual periodicity of the hydrological flow induced by IBTs is incongruent with vegetation patterns, potentially leading to shifts in the dominance of plant species (Liu et al., 2022b). Owing to distinct inter-annual patterns of groundwater table fluctuation, the unnatural flow regimes resulting from irrigation are characterized by reduced heterogeneity and vegetation diversity compared to the natural water flow (Bolpagni and Piotti, 2016). Considering the interaction between vegetation phenology and hydrological processes across scales spanning from days to centuries, employing wavelet analysis with time-scale localization and a particular applicability to non-stationary systems could provide valuable insights into the variations in time-varying flow regimes induced by IBTs and the corresponding vegetation responses across multiple time scales (Grinsted et al., 2004). The novelty of this study lies in the quantification of the influence of water transfer on the water cycle within a water-balance-constrained basin using long-term monitoring data. Additionally, we systematically analyze the changes in surface water and groundwater flow regimes across multiple time scales, including interannual, annual and seasonal, while also investigating the multiscale responses of vegetation to time-varying flow patterns.

This study was designed to address the identified knowledge gaps, with the goal of quantifying the impacts of IBTs on water balance, hydrological regimes and associated vegetation dynamics. Long-term monitoring data from a representative inland river basin, namely the

Shiyang River Basin in northwest China, were utilized for this purpose. The specific objectives of the study were to: (1) quantify the impact of IBTs on the water balance based on field observations and remote sensing data, (2) reveal the multiscale impact of IBTs on hydrological regimes using a wavelet analysis method, and (3) elucidate the response of vegetation to altered hydrological regimes resulting from IBTs.

2. Materials and methods

2.1. Study area

The Shiyang River Basin (SRB) is located in the central region of Gansu Province in northwest China (Fig. 1). The basin covers an area of 4.16×10^4 km^2 (101°41′–104°16′E and 36°29′–39°27′N) and represents a typical inland river basin characterized by alpine–oasis–desert ecosystems. SRB is located on the edge of the Asian monsoon influence, with large differences in elevation and climatic conditions within the basin. The basin spans three climatic zones from south to north: the south cold semi-arid to semi-humid zone at Qilian Mountains with an elevation of 2,000–5,000 m and an annual precipitation of 300–600 mm; the middle cool arid zone at the flatland of Hexi Corridor with an elevation of 1,500–2,000 m and an annual precipitation of 150–300 mm; the north temperate arid zone with an elevation of 500–1,500 m and an annual precipitation less than 150 mm. Orographic effects in mountains lead to differences in precipitation between mountains and lowlands, with the mean annual precipitation ranges from 821 mm in the mountains to 109 mm in the oases. The mean annual air temperature varies from –12 °C in the mountains to 9 °C in the oases at low elevations.

The Shiyang River originates from precipitation, glacial meltwater and snowmelt in the upper reaches of the Qilian Mountains and has eight tributaries. Glaciers covered an area of 30.21 km^2 (Li et al., 2016). The river eventually enters the downstream terminal lake, Qingtu Lake, which is situated between the Tengger and Badain Jaran Deserts. Qingtu Lake was dry during the period from 1960 to 2010, attributed to diminished runoff from the Shiyang River. Within the SRB, there are ten hydrology monitoring stations, and the average annual runoff volume measured at these stations is 1.67 billion m^3/y. Most of the precipitation occurs from June to September, and the total river discharge accounts for 64 % of the total annual discharge during these four months. All the tributaries of the main stream have a similar seasonal flow distribution in the basin. Zamusi (ZMS) serves as the upper control station for the Shiyang River. Caiqi (CQ) is a streamflow gauging station in the main channel of the Shiyang River. Hongyashan Reservoir (HYS), known as "Asia's Largest Desert Reservoir," is located downstream of CQ and was dry in 2004 owing to substantial midstream water demand. Jinchuanxia (JCX) is a streamflow gauging station for the tributaries of the Shiyang River. The dominant land cover type in the basin is bare land (48 %), followed by grassland (28 %) and cultivated land (17 %). However, 85 % of the water resources are used for agricultural irrigation. The per capita water resources of the SRB are 775 m^3, which is far below the internationally recognized scarcity level of 1,700 m^3.

2.2. Inter- and intra-basin transfers

To alleviate severe water shortages and restore degraded ecosystems in the lower reaches of the SRB, three major IBTs have been implemented since 2003 (Fig. 1). These include two inter-basin water transfers, namely Yin-Liu-Ji-Jin (YLJJ) and the Jingtaichuan Electric Power Irrigation Project Phase II (JDII), and one intra-basin water transfer, namely the Xiying River special canal project (XYP). YLJJ, JDII, and XYP were officially launched in 2003, 2003, and 2010, respectively. CQ receives water transferred from JDII and XYP, and JCX receives transferred water from YLJJ. YLJJ project transfers water from the Liuhuang ditch in Menyuan County of Qinghai Province, through the Qilian Mountains Lenglong Ridge into XDH of SRB, and then through the open channel to JCX downstream. The main and controlling project of YLJJ, the Lenglongling diversion tunnel, is 8.87 km long, with a designed flow of 7.5 m^3/s and an annual diversion of 40 million m^3/year. JDII project transfers water from the Yellow River via Hongshui River of SRB to CQ section through a 120.38 km desert water conveyance channel, and finally into HYS Reservoir. The designed flow rate and water transfer capacity of JDII were 6 m^3/s and 61 million m^3/year, respectively. XYP project transfers water from the Xiying River in the upper reaches of SRB to CQ through a 50.3 km channel, with a designed flow of 22 m^3/s and an annual diversion of 110 million m^3/year.

Annual and monthly water supply data for water-providing areas

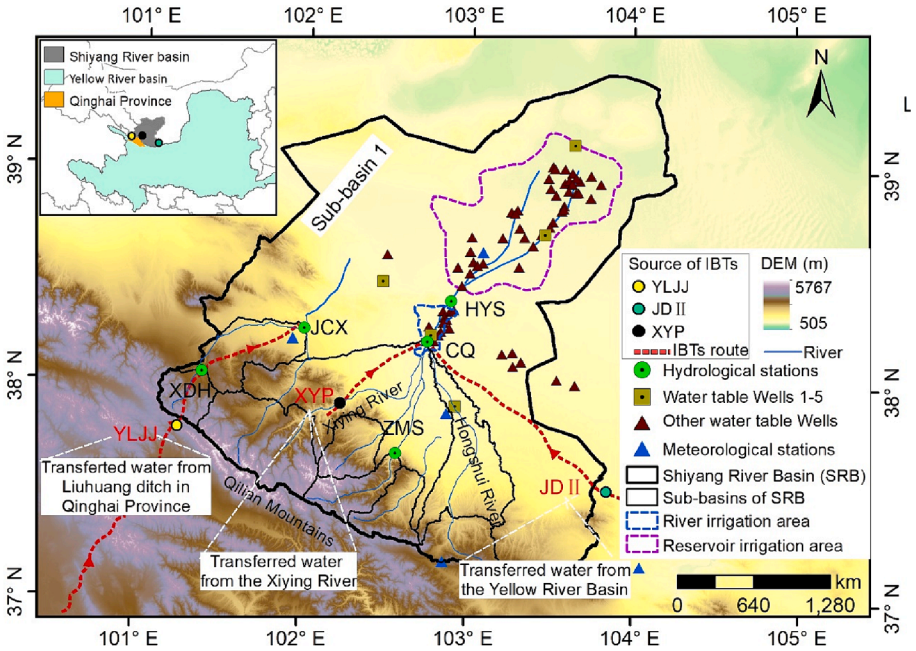

Fig. 1. Location map of the Shiyang River Basin (SRB) and the IBTs, meteorological gauging stations and groundwater Wells within the basin. Yin-Liu-Ji-Jin (YLJJ), the Jingtaichuan Electric Power Irrigation Project Phase II (JDII), and the Xiying River special canal project (XYP) are water transfer projects. ZMS, Xidahe (XDH), JCX, CQ and HYS are hydrology gauging stations with water transfer inputs.

were collected from 2003 to 2020. Considering water losses such as evaporation, seepage, and bank storage during water transfers, the actual amount of water received was calculated as follows:

$$IBT_{receiving} = IBT_{providing} \times E \quad (1)$$

where $IBT_{receiving}$ is the actual amount of water received; $IBT_{providing}$ is the amount of water supplied by water-providing areas; E is water transfer efficiency. For XYP, we obtained the $IBT_{receiving}$ and $IBT_{providing}$ of CQ section, and the average E was calculated to be 81.4 %. For YLJJ and JDII, E was obtained from the literature, which was 71.0 % (Hu, 2023) and 88.1 % (Meng, 2019), respectively.

After deducting transportation losses, the downstream SRB received a net total of 2.90 billion m^3 of water from 2003 to 2020, comprising 1.31 billion m^3 of inter-basin water transfers and 1.59 billion m^3 of intra-basin water transfers (Fig. 2). The main water-receiving station, CQ, received spring and autumn water transfers from JDII. Based on the implementation phases of the IBTs, the average transferred water was 84.0 million m^3/y during 2003–2009 (phase I of the IBTs) and 210.0 million m^3/y during 2010–2020 (phase II of the IBTs).

2.3. Watershed water balance

We examined ten sub-watersheds within the SRB and identified nested relationships based on the streamflow network, as illustrated in Fig. 1. The river network was delineated using a watershed digital elevation model (DEM) with a resolution of 100 m × 100 m. Our focus was on the water balance in downstream sub-watershed 1 because all of the transferred water ultimately reaches this location and is utilized here. We assume that the downstream sub-basin 1 is a closed watershed, neglecting the net input of groundwater that originated outside the surface watershed boundaries or net output of groundwater below the surface watershed boundaries. Therefore, sub-watershed 1 receives inputs from precipitation (P) and runoff from the midstream (RI), and it loses water through outputs including actual evapotranspiration (AET) and an outlet runoff (RO). Therefore, the annual water balance of sub-basin 1 can be expressed as follows:

$$\Delta S = P + RI - AET - RO \quad (2)$$

where ΔS are changes in water storage in the open water bodies, soils and groundwater; P is precipitation; AET is actual evapotranspiration; RO is runoff at the watershed outlet. It is important to note that sub-basin 1 is a desert oasis, and the river disappears within the basin, resulting in RO of zero. In this study, changes in surface water were not considered. Therefore, changes in water storage ($\Delta S = \Delta SM + \Delta G$) were estimated as changes in soil moisture (ΔSM) plus changes in groundwater storage (ΔG). Changes in groundwater storage were calculated as follows:

$$\Delta G = \Delta WT \times S_y \quad (3)$$

where ΔG are changes in groundwater storage; ΔWT are changes in water table; S_y is specific yield, expressing the space available for the gain or loss of groundwater associated with the rise or fall of a water table, respectively (Lv et al., 2021). Specific yield was estimated from a trilinear graph based on the soil texture (Johnson, 1967; Richey et al., 2015). All units were converted to mm/y.

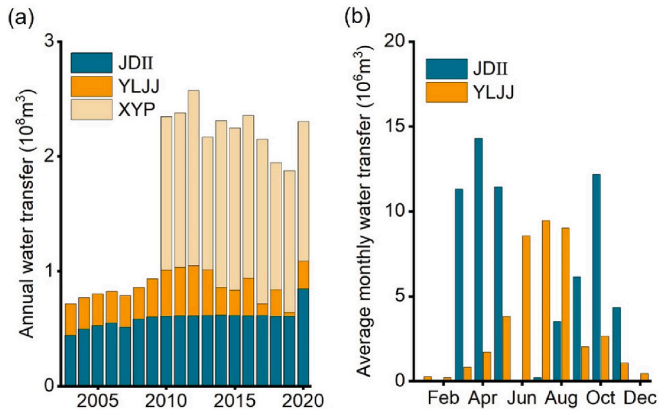

Fig. 2. Annual water transfer (a) and average monthly water transfer from JDII and YLJJ (b).

2.4. Method for periodicity analysis: Wavelet analysis and wavelet coherence

In this study, wavelet analysis was used to identify the periodicity of surface water and groundwater flow. Wavelet analysis is a common tool for breaking down time series into time–frequency space to determine the dominant modes of variability and how these modes vary in time, which has been widely used in multi-scale analysis in fields such as geophysics, hydrology, soil science, meteorology, and ecology (Cazelles et al., 2008). Ecohydrological data are usually composed of various transient processes at different scales or frequencies; therefore, they are spatially or temporally non-stationary (Su et al., 2019). Wavelet transform utilizes a series of orthogonal bases with different resolutions to represent or approximate the hydrologic signals through the expansion and translation of the wavelet basis function, so as to extract multiple time scales periodic features of the time-varying hydrologic flow signals (Guo et al., 2022). After wavelet transform, the hydrological time series was decomposed into fine-scale behavior (detailed) and large-scale behavior (approximation) (Bruce et al., 2002). High frequencies correspond to the details of changes in hydrological time series at short scales, whereas low frequencies correspond to the coarse features of slow changes in hydrological time series at long scales (Xu et al., 2013). The Matlab code for the wavelet analysis used in this study was obtained from the Wavelet Analysis Software (https://github.com/ct6502/wavelets/blob/main/wave_matlab/wavetest.m). More details of the wavelet analysis can be found in the Supplementary Materials.

Wavelet coherence was used to quantify the multi-scale relationships among surface water, groundwater, and vegetation. Traditional correlation coefficients can only provide an overview of the relationship at the sampling scale, while they conceal the characteristics of different hydrological processes across scales (Hu and Si, 2021). Wavelet coherence can overcome these limitations and quantify the degree of linear relationship between multiple factors at different time scales, which is widely accepted as a tool for detecting scale-specific and localized multiple relationships in various geoscientific domains (Grinsted et al., 2004; Su et al., 2019). More details of wavelet coherence can be found in the Supplementary Materials. The Matlab code for wavelet coherence used in this study was obtained from the Wavelet Coherence Toolbox (https://grinsted.github.io/wavelet-coherence/).

2.5. Observational and remote sensing data

Table 1 presents the key data sources, including IBTs and climate, hydrology, and vegetation data. Spatial meteorological data and groundwater depth were derived from the station data using a meteorological interpolation software (ANUSPLIN) based on spline functions developed by the Australian National University (Guo et al., 2021) and inverse distance weighting (IDW) interpolation, respectively.

3. Results

3.1. Change in the water balance under IBTs

The annual water balance of downstream sub-basin 1, which receives IBTs, was evaluated by estimating key water fluxes during the period

Table 1
A list of the key watershed and climate data sources.

Data types	Time period	Scale	Site	Data sources
IBTs	2003–2020	Monthly		Water Affairs Bureau of the SRB
Climate	1980–2020	Daily	4 within the SRB and 35 around the SRB	Meteorological gauge stations of China
River runoff	1980–2020	Monthly	10	Local hydrology gauge stations
Groundwater depth	1985–2020	Annual	5	Local groundwater gauge Wells
Groundwater depth	1999–2020	Monthly	45	Local groundwater gauge Wells
Soil moisture (0–200 cm depth)	1980–2020	Monthly and 0.25°		GLDAS-v2.1/NOAH from NASA
Soil texture	2009	1 km		Chinese Harmonized World Soil Database
Normalized Difference Vegetation Index (NDVI)	1987–2020	Monthly and 100 m		Derived from Landsat 5, 7, and 8 multispectral images provided by USGS
Water consumption	1999–2020	Annual		Gansu Water Resources Bulletin
Land use	2010	Annual		Resources and Environmental Science and Data Center of China
Digital Elevation Model (DEM)	2000	90 m		SRTM DEM from Geospatial Data Cloud of China

from 1999 to 2020 (Fig. 3). We calculated a water-balance-constrained estimation of the actual evapotranspiration (AET) using the observed precipitation (P), runoff from the midstream (RI), and groundwater depth. In the basin, about 25.8 % of the AET was derived from groundwater water storage from 1999 to 2020, resulting in a decrease in the water storage change (ΔS) at an average rate of –60.6 mm/y (groundwater storage accounting for 99.7 % of the water storage). With the implementation of the IBTs, ΔS increased significantly ($P < 0.05$, 6.4 mm/y) from –91.9 mm before the IBTs to –53.7 mm after the IBTs (–18.4 mm during phase II of the IBTs). At the same time, P and RI showed positive trends ($P > 0.05$, 1.0 mm/y and $P < 0.05$, 0.7 mm/y, respectively), whereas AET decreased significantly at a rate of 2.9 mm/y ($P < 0.05$). We further examined the relationship between AET/P and PET/P (expressing the water-relevant climate conditions in the basin). The correlation between AET/P and PET/P was only 0.32 before phase II of the IBTs, but it increased substantially thereafter (0.94).

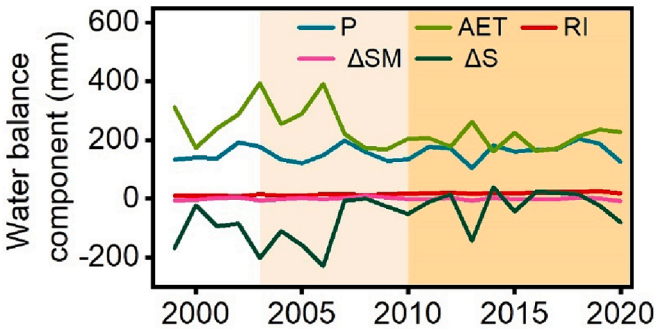

Fig. 3. Annual water balance component (mm) of sub-basin 1 in the SRB from 1999 to 2020. P is precipitation; AET is actual evapotranspiration; RI is runoff inputs from the midstream; ΔSM is change in soil moisture; ΔS is change in water storage. The light yellow and orange background refer to the phase I and phase II of the IBTs, respectively. (For interpretation of the references to color in this figure legend, the reader is referred to the web version of this article.)

We computed the climate-determined ET (ET_{clim}) using the Budyko framework model (Eq. (S4)) to segregate the contributions of RI related to IBTs and climatic conditions to the AET. ET_{clim} (156.2 mm) was far below AET (236.3 mm) and approximately equal to P (157.2 mm), which is consistent with the theoretical limit of ET = P for $PET/P > 1$. The water deficit of AET relative to climate-determined evapotranspiration (denoted as $ET_{defi} = AET - ET_{clim}$) was influenced by the RI related to IBTs and water storage. When $ET_{defi} > RI$, water storage was consumed for evapotranspiration, resulting in a negative ΔS. Conversely, when $ET_{defi} < RI$, the surplus RI contributing to ET_{defi} was replenished to water storage, leading to a positive ΔS. We further separated the water transfer from RI to quantify the impact of IBTs on ET_{defi} and ΔS. During phase I of the IBTs, the transferred water was entirely allocated to ET_{defi}, as ΔS was negative, and the IBTs contributed 1 %–32 % (average: 9 %) to ET_{defi} on average. During phase II of the IBTs, the IBTs contributed 5 %–31 % (average: 14 %) to the ET_{defi} for years with negative ΔS and 21 %–60 % (average: 42 %) to the water storage change for years with positive ΔS.

3.2. Changes in surface flow regimes at the water-receiving station

The streamflow data measured at CQ were selected to analyze the effects of IBTs on annual flow changes and were compared with the data measured upstream at ZMS without IBTs (Fig. 4a and d). Runoff at CQ decreased before the IBTs at a rate of –7.12 million m^3/y but increased significantly ($P < 0.05$) after the IBTs at a rate of 16 million m^3/y. A mutation in CQ was detected in 2010 (phase II of the IBTs) (Fig. S1b). In contrast, the runoff upstream at ZMS without IBTs inputs did not change significantly and continued to decline during the same period (–1.9 million m^3/y) (Fig. S1a). Compared to the natural runoff without IBTs (green line in Fig. 4d), the IBTs increased the natural runoff rate at CQ by 230 % during the period from 2003 to 2010 (from 4.7 million m^3/y to 15.5 million m^3/y).

Seasonal hydrological fluctuations were analyzed to understand how the specific timing of the IBTs affects the water flow (Fig. 2b, Fig. 4b and e). The natural flow in the upstream ZMS exhibited an evident seasonal distribution, with the flood season occurring from May to September and the non-flood season from October to April (Fig. 4b). However, there was lower water flow at CQ during the rainy season, and the peak flow occurred in spring. Spring and autumn water transfers (JDII in Fig. 2b) altered the intra-annual runoff distribution at CQ, resulting in peak runoff occurring in summer (Fig. 4e). The monthly runoff at CQ increased by an average of 118 % during the water transfer months.

Long-term seasonal and annual IBTs induced periodic changes in runoff (Fig. 4c and f). Natural runoff in the upstream ZMS showed a continuous fluctuation periodicity of 9–15 months (Fig. 4c). The corresponding center time scale was approximately 12 months. There was no significant periodicity in the runoff at CQ downstream before the IBTs owing to the non-seasonal river flow pattern (Fig. 4f). However, after 10 y of the IBTs, a continuous periodicity signal from 9 to 15 months was detected in the CQ, accompanied by scattered periodicities of 3–8 months.

3.3. Groundwater dynamics before and after IBTs

Groundwater was overexploited downstream before the IBTs, as evidenced by a monitored decrease in groundwater table ranging from 0.2 m/y to 0.8 m/y at different locations (Well 1–4 in Fig. 5a). After the IBTs, a significant inflection point in the groundwater was observed in 2011 (Fig. S1c, Sub 1 in Fig. 5a), and the average groundwater table decrease slowed from a significant decline of 0.82 m/y during phase I ($P < 0.01$) to an insignificant decline of 0.03 m/y during phase II ($P > 0.1$). At Qingtu Lake (Well 5 in Fig. 5a), the terminal lake of the Shiyang

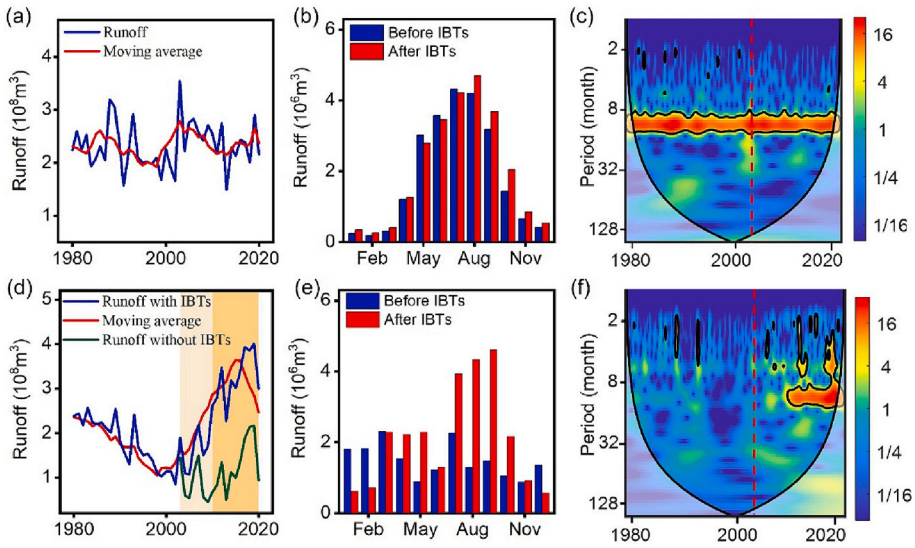

Fig. 4. Time series, intra-annual distributions and periodicity of runoff at upstream ZMS (a–c) and downstream CQ (d–f) in the SRB. (a) and (d), Annual runoff from 1980 to 2020; (b) and (e), Average monthly runoff before (1980–2002) and after (2003–2020) water transfer. (c) and (f) Periodicity of runoff from 1980 to 2020. IBTs are inter- and intra- water transfers. The light yellow and orange background of (a) and (d) refer to the phase I and phase II of the IBTs, respectively. The y-axis of (c) and (f) is the Fourier period (in month) in runoff corresponding to the wavelet scale on the right side of the heat map and the x-axis is time (year). Solid black lines indicate the 5% significance level, and the lighter shaded areas indicate the cone of influence. The red dashed lines of indicate when the water transfer began (in 2003). (For interpretation of the references to color in this figure legend, the reader is referred to the web version of this article.)

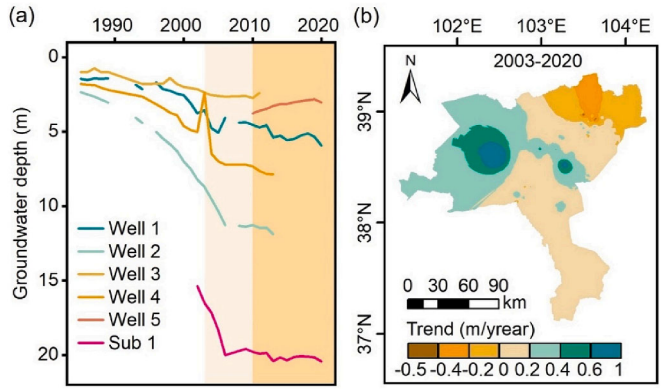

Fig. 5. Temporal (a) and spatial (b) variation of groundwater depth of sub-basin 1. Well 1–5 are water table Wells, and Sub 1 represents the average value of groundwater depth spatial interpolation in sub-basin 1. Locations of the groundwater wells can be found in Fig. 1. The light yellow and orange background of (a) refer to the phase I and phase II of the IBTs, respectively. (For interpretation of the references to color in this figure legend, the reader is referred to the web version of this article.)

River, where ecological water transfer has been implemented since 2010, the groundwater table has risen by 0.74 m (3.78 m in 2010 and 3.04 m in 2020).

Groundwater recharge characteristics, including the recharge time and amount, were altered by the IBTs (Fig. 6b and e). In the river irrigation district, the groundwater recharge pattern reversed after the IBTs, shifting from a period with little recharge to a noticeable recharge later in the growing season (July to October) (Fig. 6b). In contrast, the groundwater in the irrigation area of the reservoir remained stable both before and after the IBTs in terms of recharge timing. Notably, we observed a smaller discharge rate (from 0.77 m/month to 0.37 m/month in groundwater depth) and a faster recharge rate (from –0.21 m/month to –0.65 m/month in groundwater depth) in the reservoir irrigation area after the IBTs (Fig. 6e).

Long-term water transfer also affects groundwater recharge and periodicity. Prior to the IBTs, similar to the river flow, the groundwater near the river channel fluctuated irregularly and lacked periodicity on an annual scale (Fig. 6a and c). However, groundwater in the reservoir irrigation area exhibited continuous periodicities before the IBTs (Fig. 6d and f). After approximately 15 y of the IBTs, a new annual periodicity of 10–16 months, with altered amplitudes, emerged in both the river and reservoir irrigation areas.

3.4. Response of vegetation to hydrological change

We focused on changes in the downstream vegetation coverage, representing the final IBTs-receiving area. The annual NDVI changed markedly in 2003 (Fig. S1d) and increased significantly after 2010 ($P < 0.05$). The monthly NDVI peaked in the growing season after the IBTs, deviating from the decreasing trend observed prior to the IBTs (Fig. 7a). Positive NDVI trends were identified in 84.8 % of the total area, with agricultural land, grassland and woodland, and deserts accounting for 6.7 %, 11.6 %, and 66.3 %, respectively (Fig. S2). In the ecological water-transfer area of Qingtu Lake in the northern part of the oasis (Fig. 7b), the trend of vegetation recovery after the IBTs was most significant, aligning with the location of the rising water table (Well 5 in Fig. 5a).

The wavelet coherence between the surface water, groundwater depth, and NDVI downstream from 1999 to 2020 was used to reveal the multiple time scales and break points of their resonance period variations (Fig. 8). The highlighted regions show strong correlations at the corresponding time scales, reflecting the resonance periodicity of the ecohydrological time series. Before the IBTs (1999–2002), there were few resonance periodicities between the surface water and groundwater, indicating weak interactions between them (Fig. 8a). After the IBTs (2003–2020), the surface water and groundwater exhibited resonance periodicities on the scales of months to years (4–7 months, 8–16 months, and 22–31 months), which were more frequent and continuous particularly during phase II of the IBTs (2010–2020).

Multiple time scales and multivariate correlations between surface water, groundwater, and vegetation were also examined (Fig. 8b–d). After the IBTs (2003–2020), continuous resonance periodicities of 9–16 months and more discrete seasonal resonance periodicities of 4–8 months were detected (Fig. 8d). Compared with surface water, groundwater contributed more to vegetation greening, with a higher

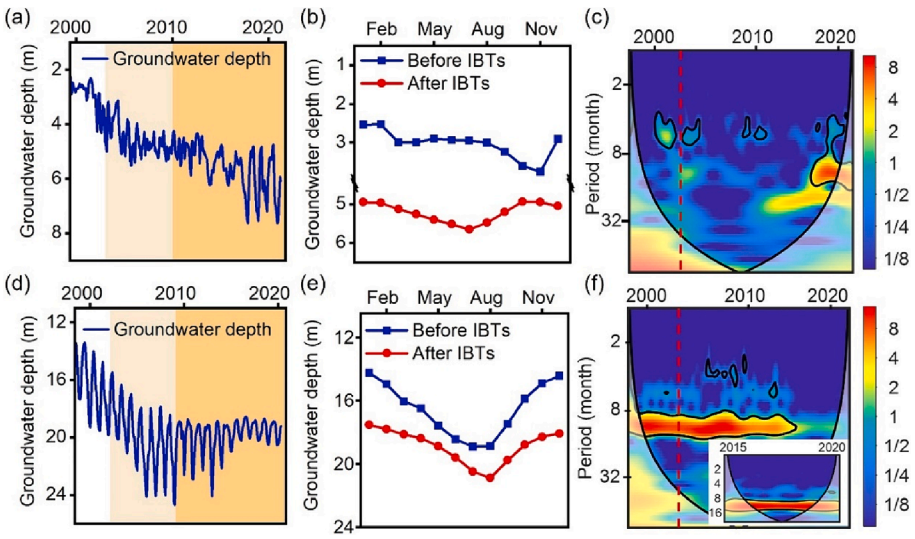

Fig. 6. Monthly variation and periodicity of groundwater depth from ground near river (a–c) and reservoir irrigation areas (d–f) from 1999 to 2020. (a) and (d), Monthly variation of groundwater depth. (b) and (e), Intra-annual distributions of groundwater depth before (1999–2002) and after (2003–2020) the IBTs. (c) and (f), Periodicity of groundwater depth. IBTs are inter- and intra- water transfers. The light yellow and orange background of (a) and (d) refer to the phase I and phase II of the IBTs, respectively. The y-axis of (c) and (f) is the Fourier period (in month) in groundwater table corresponding to the wavelet scale on the right side of the heat map and the x-axis is time (year). Solid black lines indicate the 5% significance level, and the lighter shaded areas indicate the cone of influence. The red dashed lines of indicate when the water transfer began (in 2003). The insert in (f) is the periodicity from 2015 to 2020. The location of river and reservoir irrigation areas can be found in Fig. 1. (For interpretation of the references to color in this figure legend, the reader is referred to the web version of this article.)

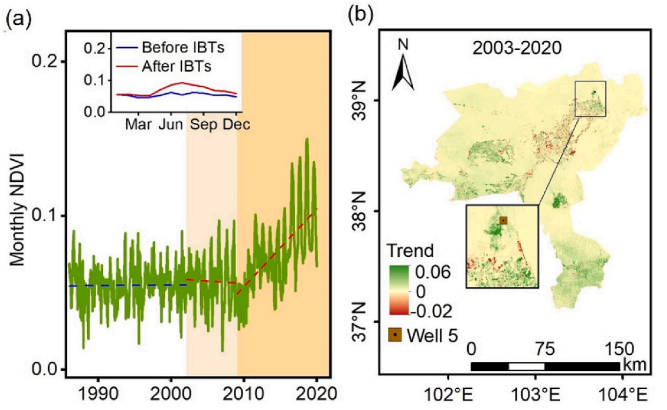

Fig. 7. Temporal and spatial variation of NDVI in sub-basin 1. (a) Monthly NDVI from 1987 to 2020. (b) Spatial trend of NDVI after water transfer (2003 to 2020). IBTs are inter-and intra-water transfers. The illustration in (a) shows the monthly average NDVI before (1987–2002) and after (2003–2020) the IBTs. The dashed lines in blue and red of (a) indicate NDVI trends before and after the IBTs, respectively. The light yellow and orange background refer to the phase I and phase II of the IBTs. (For interpretation of the references to color in this figure legend, the reader is referred to the web version of this article.)

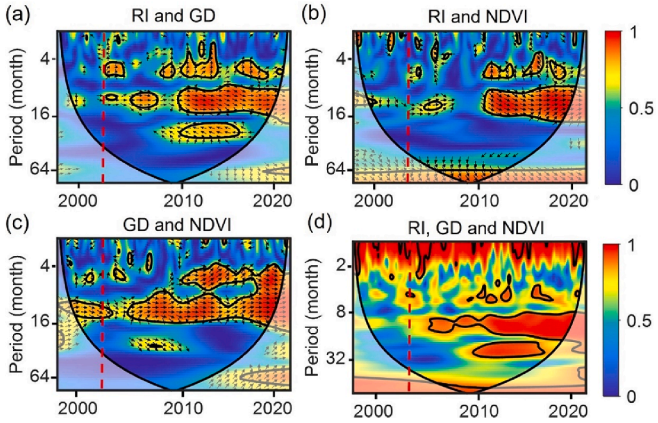

Fig. 8. Wavelet coherence between runoff input from the upstream (RI), groundwater depth (GD) and NDVI from 1999 to 2020 in sub-basin 1. (a) Bivariate wavelet coherence between RI and GD. (b) Bivariate wavelet coherence between RI and NDVI. (c) Bivariate wavelet coherence between GD and NDVI. (d) Multiple wavelet coherence between RI, GD and NDVI. The y-axis is the Fourier period (in month) of wavelet coherence and the x-axis is time (year). The color legends on the right represent the coherence coefficient, and the larger the value, the stronger the correlation. Solid black lines indicate the 5% significance level, and the lighter shaded areas indicate the cone of influence. The red dashed lines indicate when the water transfers began (in 2003). (For interpretation of the references to color in this figure legend, the reader is referred to the web version of this article.)

coherence value (0.59 in runoff, 0.61 in groundwater) and a significant coherence percentage (17.2 % in runoff, 20.2 % in groundwater) (Fig. 8b, c).

4. Discussion

4.1. Effects of IBTs on the water cycle in the inland river basin

Owing to limited precipitation but high potential evaporation in the basin, a net decline in water storage of 60.6 mm/y occurred, contributing 25.8 % of the evapotranspiration. Intensive IBTs inputs replenished the diminishing river discharge. This supplementary surface water alleviated the water constraints required for AET, thereby stabilizing the groundwater depth (the average rate of increase in the groundwater depth decreased from 0.82 m/y to 0.03 m/y). In addition, IBTs for irrigation increased the regional return flow, resulting in groundwater recharge, despite an overall loss of soil moisture (Taylor et al., 2013; Wang et al., 2018). Our study suggests that IBTs played a role in groundwater recovery, contributing 21 %–60 % (with an average of 42 %) to the increase in water storage within the basin. The recharge of groundwater by IBTs was also identified by Zhang et al. (2021). Owing to the feedback between groundwater depth and land surface water and

energy balance, alterations in IBTs-induced groundwater will subsequently impact surface fluxes and enhance the hydrological sensitivity to climate change. (Ferguson and Maxwell, 2010). The IBTs accounted for 1 %–32 % (with an average of 12 %) of the water deficit of AET relative to purely climate-determined evapotranspiration (ET_{defi} = actual evapotranspiration − climate-determined evapotranspiration). The increase in ET due to IBTs contributes to the moisture content of the air and induces surface cooling, thus potentially affecting the temperature and precipitation in the basin (Chauhan et al., 2023). Some previous studies modeled the influences of IBTs on the water and energy balance (Chauhan et al., 2023; Chen and Xie, 2010). The results revealed that IBTs led to an increase in soil moisture, latent heat flux, and precipitation, and a decrease in the average temperature in local areas. In addition, IBTs had an unexpected effect on neighboring basins through land–atmosphere feedback when the amount transferred water was sufficiently. Given the magnitude of global IBTs, disturbances in hydrological processes within the receiving basin, along with feedbacks affecting regional climate patterns and hydrological processes across river basins, are likely to be significant (Liu et al., 2022a; Shumilova et al., 2018). Therefore, models that do not consider the impact of IBTs are inadequate for quantifying the response of the water cycle to human perturbations and climate change.

4.2. Impact of IBTs on multiscale hydrological regimes

Generally, natural hydrological systems exhibit regular periodicities compatible with the local climate across various scales, including seasonal, annual, and interannual frequencies (Sivakumar, 2017). However, the persistent decline in river flow induced by human activities has resulted in the disappearance of periodicity and an intra-annual distribution characterized by low flows downstream in the summer. IBTs effectively reinstated the ubiquitous annual periodicity of six months of higher average flow and six months of lower average flow by increasing and regulating the water flow. The peak river flow shifted from late winter and early spring (February to April) to summer (July to September), thereby replenishing the reservoirs to fulfill the irrigation water demand during the growing season. Although changes in the physical processes of land-surface hydrology driven by climate change can also advance or delay the timing of annual peak runoff, the temporal range is usually no more than 2–5 weeks (Xu et al., 2021). Similarly, in other basins, IBTs have notably transformed seasonal flow patterns and periodicity. For example, the implementation of IBTs in the Heihe River Basin substantially increased the peak monthly runoff and delayed it by one month (Zhang et al., 2018). In the Tarim River Basin, the restored river flow exhibited seasonal periodicity in winter rather than during the flood season, and the annual periodicity was found to be unstable (Liu et al., 2022b).

The seasonal groundwater recharge near the river channel also changed after IBTs as a result of interactions between the surface water and groundwater (Yuan et al., 2020), causing the minimum recharge period to occur later in the growing season (July to October). After 15 y of the IBTs, the groundwater exhibited a new periodicity of 10–16 months, indicating the establishment of a new equilibrium. In addition, the attribution of evapotranspiration to climatic conditions was strengthened after long-term IBTs, as evidenced by a substantial increase in the AET/P and PET/P correlations, from 0.32 to 0.94. This evidence indicates that IBTs significantly changed the multi-scale hydrological regimes and played a positive role in restoring natural hydrological conditions through flow regulation. Downstream environments are affected by flow regulation patterns, which also offer opportunities for mitigating degradation (Lytle and Poff, 2004; Palmer and Ruhi, 2019). Indeed, practices are already in place that have restored more natural flow regimes by designing and managing river flows, yielding positive ecological and economic outcomes (Rood et al., 2005; Rood et al., 2003; Sabo and Post, 2008). In the future, watershed systems should be managed toward natural hydrological regimes, thus incorporating natural flow patterns into ecosystem and water management.

4.3. Response of vegetation to hydrological regimes altered by IBTs

Vegetation communities in dryland regions depend heavily on flow regimes of surface water and groundwater (Diehl et al., 2020; Stromberg et al., 2007). After IBTs, the recharge of surface water and ground water sources, along with the restoration of hydrological regimes, facilitates the preservation of key ecological processes such as recruitment and succession, thereby contributing to the restoration of vegetation (Rohde et al., 2021). Groundwater recharge during the late growing season after IBTs led to an increase in vegetation greenness. This occurred because vegetation exhibits a stronger dependence on groundwater during this period, characterized by the highest vapor pressure deficit and low soil moisture (Rohde et al., 2021). We observed a significant correlation between vegetation greenness and surface water and groundwater regimes at multiple time scales after the IBTs, ranging from monthly to interannual. This underscores the complex response of vegetation to hydrological regimes altered by IBTs. An example of the vegetation response is the alteration in the distribution pattern around the terminal lake, transitioning from a continuous distribution of xerophytes to a gradient distribution of hygrophytes to xerophytes (Chunyu et al., 2019). This occurred because the interactions between surface water and groundwater were enhanced on multiple time scales after IBTs, exhibiting diversified hydrologic resonance periodicity. These dynamics strongly affect the diversity and structure of plant communities (Bolpagni and Piotti, 2016; Palmer and Ruhi, 2019; Stromberg et al., 2005). Specifically, perennials prefer continuous annual periodicity with predictable and relatively stable flow regimes, whereas some annuals can respond to shorter water flow periodicity by increasing their stress tolerance (Lytle and Poff, 2004; Palmer and Ruhi, 2019; Stromberg et al.,2005). Despite the positive response of vegetation to human-regulated hydrological regimes in this study, it is still necessary to be vigilant against excessive human disturbance because watershed systems reliant on anthropogenically altered flow regimes may be more vulnerable to sudden hydrological and climate changes (Rohde et al., 2021).

4.4. Uncertainties and limitations

All components of the water balance, including water inputs, outputs, and storage changes, are expected to have substantial uncertainty at the watershed scale (Kampf et al., 2020). In this study, the actual evapotranspiration was estimated using the monitored precipitation, runoff, and groundwater depth, combined with soil moisture data from GLDASv2.1/Noah. Due to the limited number of meteorological stations within the watershed, we additionally employed data from 35 surrounding stations for spatial interpolation to reduce errors in precipitation. Water storage in the basin included surface water, near-surface soil moisture, and groundwater. Ignoring changes in surface water storage, such as reservoirs and lakes, may lead to an underestimation of storage changes, as the water area of reservoirs and lakes expands in the basin (Guo et al., 2021). Soil moisture data with a coarse resolution of 0.25° introduced uncertainty into the results, although changes in soil moisture accounted for a small proportion (0.3 %) of the total water storage change (ΔS). The groundwater storage change was calculated by multiplying the water table change by the specific yield. The primary source of uncertainty in this calculation arises from the specific yield, which is an empirical value obtained from the literature (Richey et al., 2015). We compared the water-table-derived ΔS with the GRACE-derived ΔS. There was a poor correlation (0.23) and substantial difference (–42.7 mm/y vs. 0.28 mm/y) between the two series (Fig. S3). Zhang et al. (2021) reported an opposing trend in groundwater storage compared to Wells and GRACE in areas affected by IBTs (1.8 mm/y and –16.6 mm/y). We further used three annual AET remote sensing products, namely Global Land Evaporation Amsterdam Model v3.3a

(ET_{GLEAM}), TerraClimate (ET_{TC}), and complementary relationship (ET_{CR}), for comparison with the water-balance-constrained AET (ET_{WB}) (Fig. S4). ET_{WB} had a correlation of 0.4 with ET_{CR} and almost no correlation with the other two models (<0.1). Additionally, ET_{WB} displayed a decreasing trend, in contrast to the increases in ET_{GLEAM} and ET_{TC}. Notably, the agricultural water consumption in the basin decreased at a rate of 10.73 million m^3/y (Fig. S5), which indicates the credibility and reasonableness of the results. In fact, the transferred water was concentrated in the oases of the basin, but was averaged over the entire basin area in the calculations, potentially leading to an underestimation of the contribution of the IBTs to local hydrological components. The substantial differences across data types highlight the need for long-term monitoring.

5. Conclusions and implications

Our water balance analysis revealed that IBTs projects altered hydrological components, resulting in significant changes in the seasonal distribution and periodicity of runoff and groundwater in a large inland river basin. The increased water supply and altered hydrological process promoted the establishment of vegetation, particularly during the growing season. Vegetation, surface water and groundwater exhibited multiscale resonance periodicity after the IBTs, indicating a non-negligible contribution of the IBTs to water recharge and vegetation restoration in the dryland basin.

We conclude that IBTs play a significant role in water cycles and vegetation change in arid environments, likely affecting all aspects of local ecosystems. The responses of ecohydrological systems should be continuously monitored to evaluate the sustainability of IBT projects. Future studies should also consider the impacts of IBTs on the donor watersheds to comprehensively assess the value of IBTs for meeting both human and ecosystem water needs, as well as the sustainability of IBT projects. Such information is essential for developing a decision support system that incorporates IBTs and ecohydrological models for comprehensive assessment and decision-making.

CRediT authorship contribution statement

Lin Wang: Writing – review & editing. **Wei Wei:** Writing – review & editing, Resources, Funding acquisition. **Ge Sun:** Writing – review & editing, Methodology. **Bojie Fu:** Editing. **Liding Chen:** Editing. **Xiaoming Feng:** Editing. **Philippe Ciais:** Editing. **Bhaskar Mitra:** Editing. **Lixin Wang:** Editing.

Declaration of competing interest

The authors declare that they have no known competing financial interests or personal relationships that could have appeared to influence the work reported in this paper.

Data availability

Data will be made available on request.

Acknowledgments

This research was jointly supported by the National Natural Science Foundation of China (41991233), and the Distinguished Membership Project of the Youth Innovation Promotion Association of CAS.

Appendix A. Supplementary material

Supplementary material to this article can be found online at https://doi.org/10.1016/j.jhydrol.2024.131234.

References

Abbott, B.W., Bishop, K., Zarnetske, J.P., Minaudo, C., Chapin, F.S., Krause, S., et al., 2019. Human domination of the global water cycle absent from depictions and perceptions. Nat. Geosci. 12 (7), 533–540. https://doi.org/10.1038/s41561-019-0374-y.

Berghuijs, W.R., Sivapalan, M., Woods, R.A., Savenije, H.H.G., 2014. Patterns of similarity of seasonal water balances: A window into streamflow variability over a range of time scales. Water Resour. Res. 50 (7), 5638–5661. https://doi.org/10.1002/2014WR015692.

Bolpagni, R., Piotti, A., 2016. The importance of being natural in a human-altered riverscape: role of wetland type in supporting habitat heterogeneity and the functional diversity of vegetation. Aquat. Conserv. Mar. Freshwat. Ecosyst. 26 (6), 1168–1183. https://doi.org/10.1002/aqc.2604.

Bruce, L.M., Koger, C.H., Jiang, L., 2002. Dimensionality reduction of hyperspectral data using discrete wavelet transform feature extraction. IEEE Trans. Geosci. Remote Sens. 40 (10), 2331–2338. https://doi.org/10.1109/TGRS.2002.804721.

Cazelles, B., Chavez, M., Berteaux, D., Ménard, F., Vik, J.O., Jenouvrier, S., Stenseth, N. C., 2008. Wavelet analysis of ecological time series. Oecologia 156 (2), 287–304. https://doi.org/10.1007/s00442-008-0993-2.

Chauhan, T., Devanand, A., Roxy, M.K., Ashok, K., Ghosh, S., 2023. River interlinking alters land-atmosphere feedback and changes the Indian summer monsoon. Nat. Commun. 14 (1), 5928. https://doi.org/10.1038/s41467-023-41668-x.

Chen, Y., Chen, Y., Xu, C., Ye, Z., Li, Z., Zhu, C., Ma, X., 2010. Effects of ecological water conveyance on groundwater dynamics and riparian vegetation in the lower reaches of Tarim River, China. Hydrol. Process. 24 (2), 170–177. https://doi.org/10.1002/hyp.7429.

Chen, F., Xie, Z., 2010. Effects of interbasin water transfer on regional climate: A case study of the Middle Route of the South-to-North Water Transfer Project in China. J. Geophys. Res. 115 (D11) https://doi.org/10.1029/2009jd012611.

Chunyu, X., Huang, F., Xia, Z., Zhang, D., Chen, X., Xie, Y., 2019. Assessing the ecological effects of water transport to a lake in Arid Regions: A case study of Qingtu Lake in Shiyang River Basin, Northwest China. Int. J. Environ. Res. Public Health 16 (1). https://doi.org/10.3390/ijerph16010145.

Condon, L.E., Atchley, A.L., Maxwell, R.M., 2020. Evapotranspiration depletes groundwater under warming over the contiguous United States. Nat. Commun. 11 (1), 873. https://doi.org/10.1038/s41467-020-14688-0.

De Vrese, P., Hagemann, S., 2018. Uncertainties in modelling the climate impact of irrigation. Clim. Dyn. 51 (5), 2023–2038. https://doi.org/10.1007/s00382-017-3996-z.

Destouni, G., Jaramillo, F., Prieto, C., 2013. Hydroclimatic shifts driven by human water use for food and energy production. Nat. Clim. Chang. 3 (3), 213–217. https://doi.org/10.1038/nclimate1719.

Diehl, R.M., Wilcox, A.C., Stella, J.C., 2020. Evaluation of the integrated riparian ecosystem response to future flow regimes on semiarid rivers in Colorado, USA. J. Environ. Manage. 271, 111037 https://doi.org/10.1016/j.jenvman.2020.111037.

Duan, K., Caldwell, P.V., Sun, G., McNulty, S.G., Qin, Y., Chen, X., Liu, N., 2022. Climate change challenges efficiency of inter-basin water transfers in alleviating water stress. Environ. Res. Lett. 17 (4), 044050 https://doi.org/10.1088/1748-9326/ac5e68.

Ferguson, I.M., Maxwell, R.M., 2010. Role of groundwater in watershed response and land surface feedbacks under climate change. Water Resour. Res. 46 (10) https://doi.org/10.1029/2009WR008616.

Grinsted, A., Moore, J.C., Jevrejeva, S., 2004. Application of the cross wavelet transform and wavelet coherence to geophysical time series. Nonlinear Process. Geophys. 11 (5/6), 561–566. https://doi.org/10.5194/npg-11-561-2004.

Guo, W., Jiao, X., Zhou, H., Zhu, Y., Wang, H., 2022. Hydrologic regime alteration and influence factors in the Jialing River of the Yangtze River, China. Sci. Rep. 12 (1), 11166. https://doi.org/10.1038/s41598-022-15127-4.

Guo, Y., Shao, J., Zhang, Q., Cui, Y., 2021. Relationship between water surface area of Qingtu Lake and ecological water delivery: A case study in Northwest China. Sustainability 13 (9), 4684. https://doi.org/10.3390/su13094684.

Hickel, K., Zhang, L., 2006. Estimating the impact of rainfall seasonality on mean annual water balance using a top-down approach. J. Hydrol. 331 (3), 409–424. https://doi.org/10.1016/j.jhydrol.2006.05.028.

Higgins, S.A., Overeem, I., Rogers, K.G., Kalina, E.A., 2018. River linking in India: Downstream impacts on water discharge and suspended sediment transport to deltas. Elementa-Sci. Anthropocene 6. https://doi.org/10.1525/elementa.269.

Hu, T.J., 2023. Analysis of water transfer efficiency and optimal utilization of water resources in sulfur diversion and gold recovery project. Groundwater 45 (03), 119–122. https://doi.org/10.19807/j.cnki.DXS.2023-03-041 (in Chinese).

Hu, W., Si, B., 2021. Technical Note: Improved partial wavelet coherency for understanding scale-specific and localized bivariate relationships in geosciences. Hydrol. Earth Syst. Sci. 25 (1), 321–331. https://doi.org/10.5194/hess-25-321-2021.

Huntington, T.G., 2006. Evidence for intensification of the global water cycle: Review and synthesis. J. Hydrol. 319 (1), 83–95. https://doi.org/10.1016/j.jhydrol.2005.07.003.

Jaramillo, F., Destouni, G., 2015. Local flow regulation and irrigation raise global human water consumption and footprint. Science 350 (6265), 1248–1251. https://doi.org/10.1126/science.aad1010.

Jasechko, S., Birks, S.J., Gleeson, T., Wada, Y., Fawcett, P.J., Sharp, Z.D., et al., 2014. The pronounced seasonality of global groundwater recharge. Water Resour. Res. 50 (11), 8845–8867. https://doi.org/10.1002/2014WR015809.

Johnson, A.I., 1967. Specific yield: compilation of specific yields for various materials (Report No. 1662D). U.S. Government Printing Office. https://doi.org/10.3133/wsp1662D.

Kampf, S.K., Burges, S.J., Hammond, J.C., Bhaskar, A., Covino, T.P., Eurich, A., et al., 2020. The case for an open water balance: Re-envisioning network design and data analysis for a complex, uncertain world. Water Resour. Res. 56 (6), e2019WR026699 https://doi.org/10.1029/2019WR026699.

Kuriqi, A., Pinheiro, A.N., Sordo-Ward, A., Garrote, L., 2020. Water-energy-ecosystem nexus: Balancing competing interests at a run-of-river hydropower plant coupling a hydrologic–ecohydraulic approach. Energ. Conver. Manage. 223, 113267 https://doi.org/10.1016/j.enconman.2020.113267.

Li, Z.X., Feng, Q., Wang, Q.J., Yong, S., Cheng, A.F., Li, J.G., 2016. Contribution from frozen soil meltwater to runoff in an in-land river basin under water scarcity by isotopic tracing in northwestern China. Global Planet. Change 136, 41–51. https://doi.org/10.1016/j.gloplacha.2015.12.002.

Liu, Q., Dai, H., Gui, D., Hu, B.X., Ye, M., Wei, G., et al., 2022b. Evaluation and optimization of the water diversion system of ecohydrological restoration megaproject of Tarim River, China, through wavelet analysis and a neural network. J. Hydrol. 608, 127586 https://doi.org/10.1016/j.jhydrol.2022.127586.

Liu, N., Dobbs, G.R., Caldwell, P.V., Miniat, C.F., Sun, G., Duan, K., et al., 2022a. Inter-basin transfers extend the benefits of water from forests to population centers across the conterminous U.S. Water Resour. Res. 58 (5) https://doi.org/10.1029/2021wr031537.

Lv, M., Xu, Z., Yang, Z.-L., Lu, H., Lv, M., 2021. A Comprehensive Review of Specific Yield in Land Surface and Groundwater Studies. J. Adv. Model. Earth Syst. 13 (2), e2020MS002270 https://doi.org/10.1029/2020MS002270.

Lynch, H.J., Grant, E.H.C., Muneepeerakul, R., Arunachalam, M., Rodriguez-Iturbe, I., Fagan, W.F., 2011. How restructuring river connectivity changes freshwater fish biodiversity and biogeography. Water Resour. Res. 47 https://doi.org/10.1029/2010wr010330.

Lytle, D.A., Poff, N.L., 2004. Adaptation to natural flow regimes. Trends Ecol. Evol. 19 (2), 94–100. https://doi.org/10.1016/j.tree.2003.10.002.

Meng, J.H., 2019. Thoughts on operation management of Jingdian Phase II water transfer project to MQ. Gansu Sci. Technol. 35 (17), 111–112+177 (in Chinese).

Pal, S., Talukdar, S., 2020. Modelling seasonal flow regime and environmental flow in Punarbhaba river of India and Bangladesh. J. Clean. Prod. 252, 119724 https://doi.org/j.jclepro.2019.119724.

Palmer, M., Ruhi, A., 2019. Linkages between flow regime, biota, and ecosystem processes: Implications for river restoration. Science 365 (6459), eaaw2087. https://doi.org/10.1126/science.aaw2087.

Pigram, J.J., 2000. Options for rehabilitation of Australia's Snowy River: An economic perspective. Regulat. Rivers-Res. Manage. 16 (4), 363–373. https://doi.org/10.1002/1099-1646(200007/08)16:4<363::Aid-rrr610>3.0.Co;2-i.

Richey, A.S., Thomas, B.F., Lo, M.-H., Famiglietti, J.S., Swenson, S., Rodell, M., 2015. Uncertainty in global groundwater storage estimates in a Total Groundwater Stress framework. Water Resour. Res. 51 (7), 5198–5216. https://doi.org/10.1002/2015WR017351.

Rohde, M.M., Stella, J.C., Roberts, D.A., Singer, M.B., 2021. Groundwater dependence of riparian woodlands and the disrupting effect of anthropogenically altered streamflow. Proc. Natl. Acad. Sci. 118 (25), e2026453118 https://doi.org/10.1073/pnas.2026453118.

Rolls, R.J., Bond, N.R., 2017. Chapter 4 – Environmental and Ecological Effects of Flow Alteration in Surface Water Ecosystems. In: Horne, A.C., Webb, J.A., Stewardson, M. J., Richter, B., Acreman, M. (Eds.), Water for the Environment, pp. 65–82, Academic Press. https://doi.org/10.1016/B978-0-12-803907-6.00004-8.

Rood, S.B., Gourley, C.R., Ammon, E.M., Heki, L.G., Klotz, J.R., Morrison, M.L., et al., 2003. Flows for floodplain forests: A successful riparian restoration. Bioscience 53 (7), 647–656. https://doi.org/10.1641/0006-3568(2003)053[0647:FFFFAS]2.0.CO;2.

Rood, S.B., Samuelson, G.M., Braatne, J.H., Gourley, C.R., Hughes, F.M., Mahoney, J.M., 2005. Managing river flows to restore floodplain forests. Front. Ecol. Environ. 3 (4), 193–201. https://doi.org/10.1890/1540-9295(2005)003[0193:MRFTRF]2.0.CO;2.

Sabo, J.L., Post, D.M., 2008. Quantifying periodic, stochastic, and catastrophic environmental variation. Ecol. Monogr. 78 (1), 19–40. https://doi.org/10.1890/06-1340.1.

Shibuo, Y., Jarsjö, J., Destouni, G., 2007. Hydrological responses to climate change and irrigation in the Aral Sea drainage basin. Geophys. Res. Lett. 34 (21) https://doi.org/10.1029/2007GL031465.

Shiklomanov, I.A., 2000. Appraisal and assessment of world water resources. Water Int. 25 (1), 11–32. https://doi.org/10.1080/02508060008686794.

Shumilova, O., Tockner, K., Thieme, M., Koska, A., Zarfl, C., 2018. Global water transfer megaprojects: a potential solution for the water-food-energy nexus? Front. Environ. Sci. 6, 150. https://doi.org/10.3389/fenvs.2018.00150.

Sivakumar, B., 2017. Characteristics of Hydrologic Systems. In: Sivakumar, B. (Ed.), Chaos in Hydrology: Bridging Determinism and Stochasticity. Springer, Netherlands, Dordrecht, pp. 29–62. https://doi.org/10.1007/978-90-481-2552-4_2.

Stromberg, J.C., Bagstad, K.J., Leenhouts, J.M., Lite, S.J., Makings, E., 2005. Effects of stream flow intermittency on riparian vegetation of a semiarid region river (San Pedro River, Arizona). River Res. Appl. 21 (8), 925–938. https://doi.org/10.1002/rra.858.

Stromberg, J.C., Beauchamp, V.B., Dixon, M.D., Lite, S.J., Paradzick, C., 2007. Importance of low-flow and high-flow characteristics to restoration of riparian vegetation along rivers in arid south-western United States. Freshw. Biol. 52 (4), 651–679. https://doi.org/10.1111/j.1365-2427.2006.01713.x.

Su, L., Miao, C., Duan, Q., Lei, X., Li, H., 2019. Multiple-wavelet coherence of world's large rivers with meteorological factors and ocean signals. J. Geophys. Res. Atmos. 124 (9), 4932–4954. https://doi.org/10.1029/2018JD029842.

Taylor, R.G., Scanlon, B., Döll, P., Rodell, M., van Beek, R., Wada, Y., et al., 2013. Ground water and climate change. Nat. Clim. Chang. 3 (4), 322–329. https://doi.org/10.1038/nclimate1744.

Wang, L., Jiao, W., MacBean, N., et al., 2022. Dryland productivity under a changing climate. Nat. Clim. Chang. 12, 981–994. https://doi.org/10.1038/s41558-022-01499-y.

Wang, J., Song, C., Reager, J.T., Yao, F., Famiglietti, J.S., Sheng, Y., et al., 2018. Recent global decline in endorheic basin water storages. Nat. Geosci. 11 (12), 926–932. https://doi.org/10.1038/s41561-018-0265-7.

Xu, D., Ivanov, V.Y., Li, X., Troy, T.J., 2021. Peak runoff timing is linked to global warming trajectories. Earth's Future 9 (8), e2021EF002083. https://doi.org/10.1029/2021EF002083.

Xu, J., Xu, Y., Song, C., 2013. An integrative approach to understand the climatic-hydrological process: A case study of Yarkand River, Northwest China. Adv. Meteorol. 2013, 272715 https://doi.org/10.1155/2013/272715.

Yuan, R., Wang, M., Wang, S., Song, X., 2020. Water transfer imposes hydrochemical impacts on groundwater by altering the interaction of groundwater and surface water. J. Hydrol. 583, 124617 https://doi.org/10.1016/j.jhydrol.2020.124617.

Zhang, C., Duan, Q., Yeh, J.-F., Pan, Y., Gong, H., Moradkhani, H., et al., 2021. Sub-regional groundwater storage recovery in North China Plain after the South-to-North water diversion project. J. Hydrol. 597, 126156 https://doi.org/10.1016/j.jhydrol.2021.126156.

Zhang, Y., Viglione, A., Blöschl, G., 2022. Temporal scaling of streamflow elasticity to precipitation: A global analysis. Water Resour. Res. 58 (1), e2021WR030601 https://doi.org/10.1029/2021WR030601.

Zhang, M., Wang, S., Fu, B., Gao, G., Shen, Q., 2018. Ecological effects and potential risks of the water diversion project in the Heihe River Basin. Sci. Total Environ. 619–620, 794–803. https://doi.org/10.1016/j.scitotenv.2017.11.037.

Zhang, Y., Xia, J., Liang, T., Shao, Q., 2010. Impact of water projects on river flow regimes and water quality in Huai River Basin. Water Resour. Manag. 24 (5), 889–908. https://doi.org/10.1007/s11269-009-9477-3.